Pergamon

European Journal of Cancer Vol. 30A, No. 10, pp. 1559–1564, 1994

0959-8049/94 $7.00+0.00

0959-8049(94)00293-2

Oestradiol Stimulates Growth of Oestrogen Receptor-Negative MDA-MB-231 Breast Cancer Cells in Immunodeficient Mice by Reducing Cell Loss

A. Friedl and V. C. Jordan

Growth stimulation by oestrogens in immunodeficient mice is characteristically restricted to tumours expressing oestrogen receptors (ER). We now describe oestrogen-stimulated growth of the ER-negative human breast cancer cell line MDA-MB-231, subclone 10A. Cell culture experiments confirmed that 10A cells are unresponsive to a wide concentration range of oestradiol (E_2) *in vitro*. Analysis of growth curves *in vivo* revealed significantly longer tumour volume doubling times for the control group than for the E_2-treated group. Cell cycle studies using *in vivo* labelling with bromodeoxyuridine (BrdU) and flow cytometric analysis showed essentially equal potential doubling times for controls and E_2-treated animals. These results suggest that E_2 reduces cell loss, rather than stimulating proliferation. E_2-stimulated growth was seen in both natural killer (NK) cell producing athymic (nude) mice and congenitally NK cell deficient beige nude mice. We conclude that E_2-induced natural killer cell suppression is an unlikely mechanism of action.

Key words: breast neoplasms, oestrogens, bromodeoxyuridine, mice, nude
Eur J Cancer, Vol. 30A, No. 10, pp. 1559–1564, 1994

INTRODUCTION

ATHYMIC (NUDE) mice are widely used as a model to study the growth of human tumours. They are particularly useful for analysing endocrine effects on hormone-dependent neoplasia, such as breast cancer.

According to the generally accepted model of oestrogen-stimulated breast cancer growth, oestrogen enters the target (tumour) cell and binds to nuclear oestrogen receptors (ER). After association of the hormone–receptor complex with specific DNA sequences (oestrogen response elements), the transcription of a specific set of genes is initiated, leading, among other events, to increased proliferation. The MCF-7 cell line is a well-characterised laboratory model for hormone-dependent human breast cancer. MCF-7 cells require oestrogen for growth *in vitro* [1] as well as for growth in athymic mice [2]. Conversely, the human breast cancer cell line MDA-MB-231 is ER-negative and serves as a prototype for hormone-independent breast cancer that demonstrates oestrogen independence *in vitro* and *in vivo*.

We have previously reported on an ER-negative human endometrial carcinoma (BR endometrial carcinoma) [3] that is serially transplantable in athymic mice. Tumour BR is tumorigenic in athymic mice without hormone treatment, but oestradiol (E_2) supplementation leads to significant growth stimulation. We hypothesised that this effect might be mediated by modulation of the animal host, namely by E_2-induced suppression of natural killer (NK) cell activity. In the case of BR, it is, however, difficult to exclude the possibility that low and undetectable levels of ER in the tumour cells may cause growth stimulation via the classic receptor-mediated pathway. Since tumour BR has not been grown in culture, a direct growth stimulation by E_2 could not be ruled out. In the present article, we extend these previous observations to the well-characterised ER-negative human breast cancer cell line MDA-MB-231. In our experiments, we used a subclone (10A) of that cell line that has a slower growth rate than wild-type MDA-MB-231 cells, but has retained ER-negativity [4]. Using nuclear run-on assays and the highly sensitive polymerase chain reaction (PCR), it has recently been shown that MDA-MB-231 cells do not transcribe the ER gene [5]. Nevertheless, we now show that E_2 has no effect on growth *in vitro* but stimulates growth *in vivo*. We have investigated one possible mechanism responsible for E_2-stimulated growth *in vivo* by using a strain of immunodeficient mice that does not have NK cells, and compared the tumour cell cycle kinetics by flow cytometric analysis with and without E_2 treatment.

MATERIALS AND METHODS

Cell line

MDA-MB-231 cells were obtained from ATCC (Rockville, Maryland, U.S.A.). Clone 10A was derived from wild-type MDA-MB-231 cells by cloning in 96-well plates at 0.5 cells/well [4]. Cells were maintained in minimal essential medium (MEM), supplemented with 5% calf serum, 1% penicillin and strepto-

Correspondence to A. Friedl. The authors are at the Robert H. Lurie Cancer Center, Northwestern University Medical School, 303 East Chicago Avenue, Olsen Pavilion 8250, Chicago, Illinois 60611-3008, U.S.A.
Revised 24 May 1994; accepted 9 June 1994.

mycin and 1% glutamine. All tissue culture media and reagents were obtained from Gibco (Gibco BRL Life Technologies, Inc., Gaithersburg, Maryland, U.S.A.).

Growth experiments in vitro

Cells were plated in 24-well plates at a density of 30 000 cells/well. On day 1, the medium was changed to phenol red-free medium substituted with charcoal-treated calf serum. From days 3 to 8, cells were exposed to 17β-E_2-containing medium (10^{-13} to 10^{-6} M) or control medium (0.1% ethanol vehicle only). Cells were harvested and lysed by sonication in calcium and magnesium-free Hanks buffered saline solution (HBSS). Total DNA was measured using fluorescence photometry with Hoechst 33258 dye (Sigma, St Louis, Missouri, U.S.A.) and the SLM-Aminco Fluoro Colorimeter III.

Animals

Female ovariectomised BALB/c athymic mice and outbred NIH Swiss beige/nude/xid mice were purchased from Harlan Sprague Dawley (Indianapolis, Indiana, U.S.A.). The animals were kept under pathogen-free conditions and were fed *ad libitum* autoclaved LM-485 chow (Teklad, Madison, Wisconsin, U.S.A.) and autoclaved water. All experiments were performed with 4–5-week-old mice.

Growth experiments in vivo

Cells were grown to confluence in 15-cm tissue culture dishes. For harvesting, medium was aspirated, dishes were rinsed with EDTA solution and cells were gently scraped off. Cells were then suspended in MEM, centrifuged and resuspended to a final concentration of 30×10^6/ml or 2×10^6/ml. Cell suspension (0.1 ml) was injected into the axillary fat pad. Treatment was started immediately by implanting a 2-cm 17β-E_2 silastic capsule or a control capsule. Tumours were measured weekly in two dimensions using a caliper. Tumour area (A) was calculated using the equation:

$$A = a \times b \times \pi/4,$$

with a being the shorter tumour axis and b being the longer. At the time of animal sacrifice, uterine weights were recorded to confirm the presence of active oestrogen.

Growth kinetics

Tumour volume (V) was calculated by assuming an ellipsoid tumour shape with the equation: $V = a^2 \times b \times \pi/6$. Assuming exponential growth, tumour volume doubling time (T_D) was derived by using the equation: $T_D = \log 2/s$, where s is the slope of a straight line in a plot of the decadic logarithm of mean tumour volume versus time. The value of s was calculated by linear regression analysis.

Cell cycle analysis

For cell cycle analysis, we used the protocol described by Ritter and colleagues [6]. Briefly, at 9 weeks the mice were injected intraperitoneally (i.p.) with 0.1 ml of a sterile 10 mg/ml BrdU solution. One mouse did not receive BrdU and served as a red control. After 7 h, animals were sacrificed, and tumours were excised, minced and fixed in 70% ethanol (in 0.15 M NaCl.) After digestion in 0.04% pepsin/0.1 N HCl for 60 min at 37°C, the suspension was filtered through a 35-μm nylon mesh. The suspensions were treated with 2 N NCl for 30 min at 30°C and then neutralised with 0.1 M sodium borate. After rinsing in phosphate buffered saline (PBS), 2×10^6 nuclei were resuspended in 50 μl PBS with 0.5% Tween 20 and 1 mg/ml bovine serum albumin and incubated with 20 μl of antiBrdU antibody (Becton Dickinson, San Jose, California, U.S.A.) at room temperature in the dark. After rinsing, the nuclei were incubated with a 1:50 dilution of the secondary antibody (antimouse– FITC conjugate, Sigma) in PBS with 0.5% Tween 20 and 1 μl/ml goat serum. Nuclei were stained with 30 μg/ml propidium iodide (PI) and simultaneously treated with RNAse (5 μg/ml). PI staining was omitted on one tumour sample (green control). Samples were stored overnight at 4°C and data were analysed with a Becton Dickinson FACScan flow cytometer, using LYSIS II V. 1.0 software. A display of red versus green fluorescence allowed gating of cells in G1/0, G2+M (PI only) and of BrdU labelled cells. Cell cycle parameters were calculated according to the method of Begg and colleagues [7]. Briefly, relative movement (R_m) was calculated using the formula:

$$R_m = (F_L - F_{G1})/(F_{GM} - F_{G1}),$$

where F_L is the mean red PI fluorescence of the green BrdU-labelled cells (region R4 in Figure 1) and F_{G1} and F_{GM} are the mean red fluorescence values of G1 and G2+M cells (regions R2 and R5 in Figure 1). DNA synthesis phase duration (T_S) was calculated using the equation:

$$T_S = 0.4 \times t/(R_m - 0.6),$$

where t is the duration of BrdU exposure. According to Begg and colleagues [7] this equation describes S-phase duration of human tumours more accurately than the more commonly applied equation:

$$T_S = 0.5 \times t/(R_m - 0.5)$$

which is based on the assumption of a relative movement of 0.5 at time zero.

LI was obtained by dividing the number of BrdU-labelled cells by the number of all cells analysed. Potential tumour volume doubling time (T_{pot}) could be derived using the formula:

$$T_{pot} = T_S/LI.$$

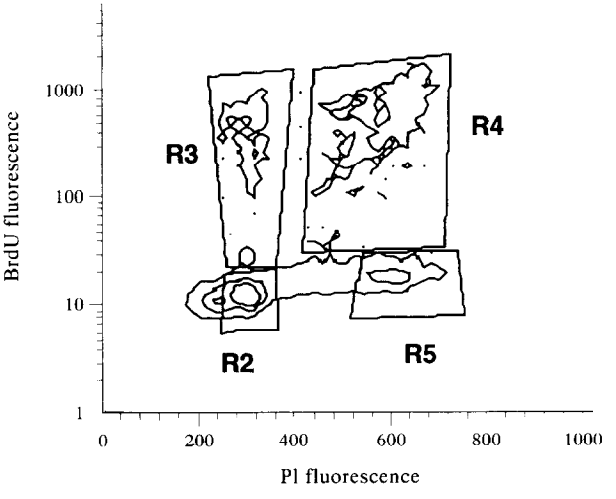

Figure 1. Cell cycle analysis with BrdU labelling. Green (BrdU) versus red (PI) fluorescence is displayed for one tumour as a frequency contour plot. Measurements are expressed as channel numbers (PI) and arbitrary intensity units (BrdU). See text for details.

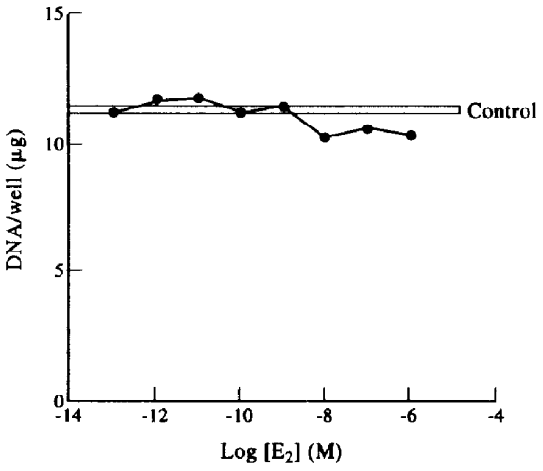

Figure 2. Oestradiol treatment of MDA-MB-231 10A cells *in vitro*. Cells were cultured for 8 days and treated with E_2 for 5 days. Each data point represents the mean of triplicates ±S.E. Error bars are too small for graphic display. The bar indicates mean ±S.E. of the control group (no E_2)

Cell loss factor (Φ) was calculated using the following formula:

$$\Phi = 1 - T_{pot}/T_D.$$

Statistics

All statistical analyses were performed with StatView 512+ software (BrainPower Inc., Calabasas, California, U.S.A.). Tumour size was compared by the Student's *t*-test. Regression analysis results for the calculation of tumour volume doubling time were compared using confidence interval calculations. Tumour incidences were compared with χ^2-test of associations.

RESULTS

In vitro *growth experiments*

Figure 2 shows *in vitro* growth of MDA-MB-231 10A cells, exposed to a wide range of E_2 concentrations. No stimulation beyond the untreated control group was demonstrated.

Influence of NK cells

Figure 3 illustrates that E_2 stimulates growth of MDA-MB-231 10A cells in athymic mice as well as in congenitally NK cell deficient beige-nude mice. Inoculum size was 3×10^6 cells. Compared with controls, tumours were significantly ($P < 0.05$) larger in E_2-treated athymic mice from 5 weeks onward and in E_2-treated beige-nude mice from 6 weeks onward. Tumour incidence did not differ significantly between control and E_2 treatment groups in athymic or in beige-nude mice. A second set of mice was inoculated with 2×10^5 cells per site. Tumour incidence was greatly reduced in controls compared with E_2-treated animals. Only one small tumour grew in each of the control groups; tumour sizes were similar in E_2-treated athymic and beige-nude mice. Tumour incidences for both inoculum sizes are summarised in Table 1. In subsequent growth experiments, beige-nude mice were used to exclude the influence of NK cells.

Table 1. Incidence of MDA-MB-231 10A tumours (number of tumours per total number of inoculation sites per group after eight weeks)

Inoculum size (cells/site)	Animals	Control	E_2
3×10^6	Athymic	6/7	6/7*
	Beige-nude	4/6	4/5*
2×10^5	Athymic	1/12	9/12†
	Beige-nude	1/12	4/8‡

* Difference non-significant. † Difference significant ($P = 0.0009$). ‡ Difference significant ($P = 0.035$).

Tumour growth kinetics

In a different growth experiment, 12 mice per group were inoculated with 3×10^6 cells bilaterally. Mean tumour area was significantly larger in E_2-treated animals from week 5 onward. Tumour incidence was 23/24 sites for control and 20/20 sites in E_2-treated mice (two mice died in this group). Proper release of E_2 from the capsules was confirmed by measurement of uterine weights. The mean uterine weight was 6.43 mg (±0.9 S.E.) in the control group and 88.8 mg (±13.3 S.E.) in E_2-treated animals. Figure 4 shows the decadic logarithm of tumour volume versus time, allowing linear regression analysis and calculation of T_D (see Materials and Methods). Correlation coefficients *r*

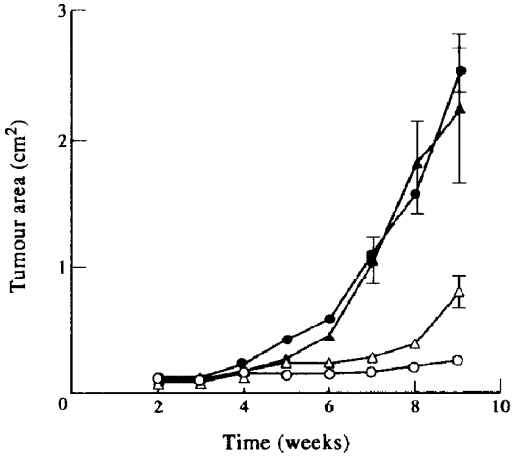

Figure 3. Growth of MDA-MB-231 10A cells in athymic (circles) and beige-nude mice (triangles). Animals were treated either with 2 cm E_2 capsules (closed symbols) or with sham implants (open symbols). Each data point represents mean tumour area ±S.E. *$P < 0.05$.

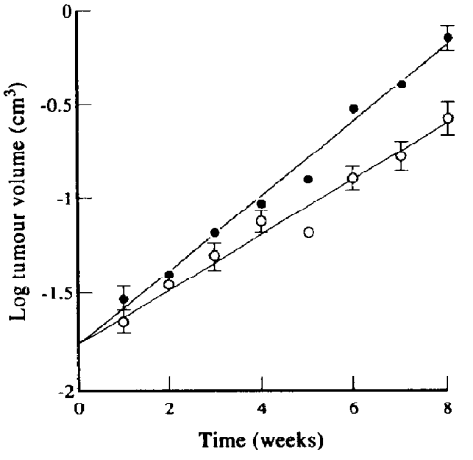

Figure 4. Mean tumour volume of MDA-MB-231 10A cells grown in beige-nude mice displayed in logarithmic form. Animals were either treated with 2 cm E_2 capsules (closed circles) or sham implants (open circles). The lines indicate least squares fits.

Table 2. Tumour growth kinetics and cell cycle analysis: results are expressed as means ±S.E. or 95% confidence intervals (in parentheses)

Parameters	Control	E_2
LI (%)	7.9 ± 0.40	9.3 ± 0.25*
T_S (h)	10.5 ± 0.20	12.4 ± 0.43*
T_{pot} (h)	146.9 ± 7.7	147.8 ± 8.6*
T_D (h)	341.7 (292.3–414.5)	249.1 (228.8–279.4)†
ϕ	0.57	0.41

* Difference statistically non-significant. † Difference statistically significant ($P < 0.05$).

were 0.985 for the control group and 0.994 for the E_2 group. The slope s of the linearised growth curve was 0.148 for control tumours and 0.203 for E_2-treated tumours, with 95% confidence intervals ranging from 0.122 to 0.173 and from 0.181 to 0.221, respectively. From these values, a T_D of 341.7 h was calculated for the control group and of 249.1 h for the E_2 group. Cell cycle analysis was performed in order to assess proliferative activity. Figure 1 shows flow cytometric results of a single tumour. Singlet events are depicted as frequency contour plot. We were able to distinguish four distinct subpopulations. The gated regions R2 and R5 represent cells in G0 and unlabelled cells in G2/M phase of the cell cycle, respectively. Region R4 represents BrdU-labelled cells in S and G2/M phase, region R3 labelled cells in G1 after undergoing mitosis. The small population located to the left of R2 consists of normal mouse cells. Percentages of cells in the different gates and relative movement values allow calculation of the proliferating pool (expressed as LI), T_S and T_{pot} (see Materials and Methods). Results of nine tumours per group are summarised in Table 2, together with actual tumour growth parameters for all tumours. LI was found to be slightly larger in the E_2-treated group but T_S was slightly shorter in the control group. The differences were statistically nonsignificant. Potential doubling times were almost identical. Φ was derived by comparing T_D and T_{pot} and was larger in control tumours (0.57) than in E_2-treated tumours (0.41). Since the values of Φ were determined indirectly from mean tumour volume measurements, it was not possible to test the difference for statistical significance.

DISCUSSION

We have previously described E_2-stimulated growth of the ER-negative endometrial carcinoma BR [3] in athymic mice. With our results on MDA-MB-231 10A cells, we demonstrate that E_2-stimulated growth of ER-negative tumours in immunodeficient animals is not an isolated phenomenon restricted to the endometrial carcinoma BR. We observed a sustained growth promoting effect of E_2 on the ER-negative breast tumours. When small inoculum sizes were used, E_2 greatly enhanced tumour take. As expected for ER-negative cells, E_2 has no effect on growth of MDA-MB-231 10A cells *in vitro*. These results strongly suggest an animal host-mediated mechanism of action. The list of possible explanations is long and includes modulation of the immune system, of endocrine or paracrine growth factors, or alteration of the tissue matrix. Our experiments were designed to eliminate some of these possibilities and further narrow the scope in future experiments to discover the mechanism of oestrogen action as a tumour growth promoter.

Growth and cell cycle kinetics

In our experimental model, E_2 treatment leads to shorter tumour doubling times, suggesting a sustained growth promoting effect. Accelerated growth could be due to an increase in proliferation, or a decrease in cell loss. Using *in vivo* labelling with BrdU and flow cytometric analysis, we demonstrated equal potential doubling times in either treatment group. We conclude from these data that E_2 reduces cell loss in MDA-MB-231 10A tumours. The calculated cell loss factors of 0.57 and 0.41 are at the lower end of the range reported for human malignancies [8, 9]. The cell loss factor has been shown to increase with tumour size [9]. Even though tumours were approximately twice as large in E_2-treated mice, Φ was larger in the control group. We hypothesise that E_2 exerts its effect by reducing apoptosis, which is considered the single most important factor contributing to tumour cell loss [8]. To date, we have not obtained direct evidence to prove this hypothesis. The cascade of events in apoptosis includes initiation of the process through external or possibly internal signals. The list of alleged triggering stimuli is long and includes chemotherapeutic agents, radiation, killer cell action and growth factor or hormone withdrawal (reviewed in [10]). Interestingly, within the experimental model of *N*-nitrosomorpholine-induced rat liver tumours, treatment with the promoter, phenobarbital, leads to accelerated growth also by reducing apoptosis rather than increasing cell replication [11].

To our knowledge, E_2-stimulated growth of rapidly growing wild-type MDA-MB-231 cells had not been reported. We selected clone 10A for its relatively slow growth rate that was comparable with growth of endometrial carcinoma BR. We suspect that the growth-promoting effect of E_2 is dependent on slow baseline growth, although we have not investigated this hypothesis systematically.

Since our observations of growth kinetics were limited to relatively small tumours, it was unnecessary to apply complex Gompertzian models because increases in tumour volume were well described by a simple exponential equation.

Immune system

Components of the immune system thought to be involved in tumour surveillance, tumour regression and elimination of tumour cells from the blood stream are cytotoxic T cells and NK cells. Athymic nude mice are successfully used as hosts for human tumours because they lack immunocompetent T cells. They do, however, produce NK cells, which are present in elevated numbers compared with related strains without thymus aplasia [12]. E_2 has been shown to suppress NK activity in mice [13] and reduced NK activity is associated with increased metastatic potential of different human cell lines in athymic mice [14]. Similarly, other investigators [15] showed that reduction of NK activity with specific antibodies can lead to enhanced growth of human tumours in athymic animals. However, mice with the beige mutation lack functional NK cells [16] and hybrid beige-nude mice are also devoid of immunocompetent T cells [17]. In previous experiments performed in our laboratory, we could not demonstrate any detectable NK activity in beige-nude mice of identical lineage [18]. In order to test the influence of NK cells on growth of MDA-MB-231 10A cells, we compared their growth in athymic and in beige-nude mice. Not only was the growth rate comparable in both strains of mouse but, more importantly, E_2-stimulated growth was maintained in NK deficient beige-nude mice. These findings argue strongly against a NK cell mediated mechanism of action. Our observations are in agreement with those of other authors who could not

demonstrate a correlation between growth control of human tumours and natural killer cell activity in athymic mice with different immune defects [19].

Tumour stroma

Kawatsu and coworkers [20] observed increased tumour take and earlier tumour development in oestriol-treated ER-negative lymphoma cells grown in syngeneic mice. Oestriol-enhanced tumorigenesis was accompanied by higher levels of hyaluronic acid in the skin of the animals. In contrast to our results, these investigators saw no difference in tumour growth rate.

Potentially, E_2 treatment could enhance angiogenesis, resulting in increased growth. To our knowledge, there are no reports in the literature, supporting such an oestrogen effect on tumour stroma.

Growth factors

Treatment of breast cancer patients with the anti-oestrogen tamoxifen leads to production of transforming growth factor (TGF)-β_1 by stromal fibroblasts [21]. TGF-β_1 has a growth-inhibiting effect on epithelial cells. Conversely, E_2 treatment could induce stromal cells to secrete paracrine growth stimulatory factors.

Alternatively, E_2 treatment could induce an endocrine second messenger, such as growth hormone (GH), and subsequently IGF-1. Simard and colleagues [22] demonstrated that E_2 induced GH synthesis and release in cultured rat pituitary cells. Interestingly, blockade of type I insulin-like growth factor (IGF) receptors with a monoclonal antibody results in growth suppression of MDA-MB-231 cells in athymic mice [23].

In summary, our results show that E_2 treatment can enhance growth and tumour take of ER-negative breast cancer cells in immunodeficient mice. We were further able to show that this growth stimulation is due to a reduction in cell loss that is independent of NK cell activity.

E_2-induced growth stimultion in athymic mice has been used as evidence for hormone dependency of primary human tumours [24]. Our experience [25] suggests that such observations should be interpreted with caution. Human tumours in immunodeficient host animals represent a complex model; steroid hormones modulate the residual immune system, influence the endocrine milieu and alter the connective tissue matrix within the tumour and in its vicinity. Conversely, the athymic mouse model provides us with an opportunity to study these host-tumour interactions that may be of significance for human neoplasia.

Initiated by a report by Hrushesky and coworkers [26], there has been an ongoing debate on the effect of timing of surgery within the menstrual cycle on the prognosis of premenopausal women with breast cancer. The initial observation that surgery during the time of oestrogen dominance is associated with poor outcome was disputed by other groups [27, 28]. A prospective trial [29] with 283 patients found a statistically higher recurrence rate among patients who had their primary tumour removed during the follicular phase as compared with those who underwent surgery later in the cycle. Hrushesky's results are also supported by a recent meta-analysis [30]. It has been suggested that higher levels of oestrogens unopposed by progestins somehow facilitate the establishment of micrometastases at the time of surgery. We speculate that our observation of increased tumour take and increased growth rate in E_2-treated mice could be mediated by the same unknown mechanism.

1. Lippman M, Bolan G, Huff K. The effects of estrogens and antiestrogens on hormone-responsive human breast cancer in long-term tissue culture. *Cancer Res* 1976, **36**, 4595–4601.
2. Shafie SM, Grantham FH. Role of hormones in the growth and regression of human breast cancer cells (MCF-7) transplanted into athymic nude mice. *J Natl Cancer Inst* 1981, **67**, 51–56.
3. Friedl A, Gottardis MM, Pink J, Buchler DA, Jordan VC. Enhanced growth of an estogen receptor-negative endometrial adenocarcinoma by estradiol in athymic mice. *Cancer Res* 1989, **49**, 4758–64.
4. Jiang SY, Jordan VC. Growth regulation of estrogen receptor-negative breast cancer cells transfected with complementary DNAs for estrogen receptor. *J Natl Cancer Inst* 1992, **84**, 580–91.
5. Weigel RJ, deConnick EC. Transcriptional control of estrogen receptor in estrogen receptor-negative breast carcinoma. *Cancer Res* 1993, **53**, 3472–3474.
6. Ritter MA, Fowler JF, Kim Y, Lindstrom MJ, Kinsella TJ. Single biopsy, tumor kinetic analyses: a comparison of methods and an extension to shorter sampling intervals. *Int J Radiat Oncol Biol* 1992, **23**, 811–20.
7. Begg AC, McNally NJ, Shrieve DC, Kärcher H. A method to measure the duration of DNA synthesis and the potential doubling time from a single sample. *Cytometry* 1985, **6**, 620–626.
8. Wyllie AH. The biology of cell death in tumours. *Anticancer Res* 1985, **5**, 131–136.
9. Spang-Thomsen M, Vindeløv LL. Proliferation kinetics of a human malignant melanoma serially grown in nude mice. *Cell Tissue Kinet* 1984, **17**, 401–410.
10. Carson DA, Ribeiro JM. Apoptosis and disease. *Lancet* 1993, **341**, 1251–1254.
11. Schult-Herrmann R, Timmermann-Trosiener I, Barthel G, Bursch W. DNA synthesis, apoptosis, and phenotypic expression as determinants of growth of altered foci in rat liver during phenobarbital promotion. *Cancer Res* 1990, **50**, 5127–5135.
12. Herberman RB, Holden HT. Natural cell-mediated immunity. In Klein G and Weinhouse S, eds. *Advances in Cancer Research*. Academic Press, New York, 1978, 305–377.
13. Seamen WE, Blackman MA, Gindhart TD, Roubinian JR, Loeb JM, Talal N. Beta-estradiol reduces natural killer cells in mice. *J Immunol* 1978, **121**, 2193–2198.
14. Kozlowski JM, Fidler IJ, Campbell D, Xu ZL, Kaighn ME, Hart IR. Metastatic behavior of human tumor cell lines grown in the nude mouse. *Cancer Res* 1984, **44**, 3522–9.
15. Habu S, Fukui H, Shimamura K, Kasai M, Nagai Y, Okumura K, Tamaoki N. *In vivo* effects of anti-asialo GM1: 1. Reduction of NK activity and enhancement of transplanted tumor growth in nude mice. *J Immunol* 1981, **127**, 34–38.
16. Roder J, Duwe A. The beige mutation in the mouse selectively impairs natural killer cell function. *Nature* 1979, **278**, 451–453.
17. Fodstad Ø, Hansen CT, Cannon GB, Boyd MR. Immune characteristics of the beige-nude mouse: a model for studying immune surveillance. *Scand J Immunol* 1984, **20**, 267–272.
18. Gottardis MM, Wagner RJ, Borden EC, Jordan VC. Differential ability of antiestrogens to stimulate breast cancer cell (MCF-7) growth *in vivo* and *in vitro*. *Cancer Res* 1989, **49**, 4765–9.
19. Fodstad Ø, Hansen CT, Cannon GB, Statham CN, Lichtenstein GR, Boyd MR. Lack of correlation between natural killer cell activity and tumor growth control in nude mice with different immune defects. *Cancer Res* 1984, **44**, 4403–4408.
20. Kawatsu R, Ezaki T, Kotani M, Akagi M. Growth-promoting effect of oestradiol in a lymphoma lacking oestrogen receptors. *Br J Cancer* 1989, **59**, 563–568.
21. Butta A, MacLennan K, Flanders KC, *et al.* Induction of transforming growth factor beta 1 in human breast cancer in vivo following tamoxifen treatment. *Cancer Res* 1992, **52**, 4261–4.
22. Simard J, Hupert J-F, Hosseinzadeh T, Labrie F. Stimulation of growth hormone release and synthesis by estrogens in rat anterior pituitary cells in culture. *Endocrinology* 1986, **119**, 2004–2011.
23. Arteaga CL, Kitten LJ, Coronado EB, Jacobs S, Kull FJ, Allred DC, Osborne CK. Blockade of the type I somatomedin receptor inhibits growth of human breast cancer cells in athymic mice. *J Clin Invest* 1989, **84**, 1418–23.
24. Somers KD, Koenig M, Schechter GL. Growth of head and neck squamous cell carcinoma in nude mice: potentiation of laryngeal carcinoma by 17 beta-estradiol. *J Natl Cancer Inst* 1988, **80**, 688–91.
25. Jordan VC, Gottardis MM, Robinson SP, Friedl A. Immune-

deficient animals to study "hormone-dependent" breast and endometrial cancer. *J Steroid Biochem* 1989, **34**, 169–76.
26. Hrushesky WJ, Bluming AZ, Gruber SA, Sothern RB. Menstrual influence on surgical cure of breast cancer. *Lancet* 1989, 2, 949–952.
27. Powles TJ, Jones AL, Ashley S, Tidy A. Menstrual effect on surgical cure of breast cancer [letter]. *Lancet* 1989, 2, 1343–1344.
28. Gelber RD, Goldhirsch A. Menstrual effect on surgical cure of breast cancer. *Lancet* 1989, 2, 1344.
29. Senie RT, Rosen PP, Rhodes P, Lesser ML. Timing of breast cancer excision during the menstrual cycle influences duration of disease-free survival. *Ann Intern Med* 1991, **115**, 337–342.
30. Gregory WM, Richards MA, Fentiman IS. Optimal timing of initial breast surgery [Letter]. *Ann Intern Med* 1992, **116**, 268–269.

Acknowledgements—We thank Ms Kathleen Schell for excellent technical assistance with the flow cytometric analysis. This research is supported by NIH grant CA-14520.

Pergamon

European Journal of Cancer Vol. 30A, No. 10, pp. 1564–1570, 1994

0959-8049/94 $7.00+0.00

0959-8049(94)00291-6

A Novel Microculture Kinetic Assay (MiCK Assay) for Malignant Cell Growth and Chemosensitivity

V.D. Kravtsov

The THERMOmax™ microplate reader was adapted for monitoring the growth kinetics of human leukaemic OCI/AML-2 and mouse tumour J-774.1 cell lines in continuous culture. Fluid evaporation from wells, CO_2 escape and contamination were prevented by hermetic sealing of the microcultures in wells of a 96-well microplate, thus enabling the cells to grow exponentially for 72 h under the conditions of the incubated microplate reader. For both OCI/AML-2 cells, which grow in suspension, and adherent J-774.1 cells, a linear correlation was demonstrated between the number of unstained cells seeded in a given microplate well and the optical density (OD) of that well. Therefore, the OD/time curve of the culture could be deemed to be its growth curve. By the use of the linear fit equation, the actual number of the cells in the wells was computable at any time point of the assay. In the chemosensitivity test, an inhibitory effect of ARA-C on the growth of the cells could be estimated by viewing of the growth curves plotted on the screen. The maximum kinetic rates (*V*max) of the curves in the control and the ARA-C-treated wells were compared, yielding a growth inhibition index (GII). Comparison of results of the kinetic chemosensitivity assay with those of a [^{3}H]thymidine incorporation assay revealed that the novel assay is suitable for precise quantitation of the cell chemosensitivity, is more informative and has the added technical advantage of performance without recourse to radioactive or chemically hazardous substances.

Key words: malignant cells, growth kinetics, chemosensitivity
Eur J Cancer, Vol. 30A, No. 10, pp. 1564–1570, 1994

INTRODUCTION

SEVERAL SPECTROPHOTOMETRIC non-clonogenic microculture assays have been developed to determine proliferation and chemosensitivity of malignant cells *in vitro*. These make use of tetrazolium-based colorimetric assay [1–6] or fluorimetric microculture cytotoxicity assay [7, 8], both of which are convenient for handling a large number of samples. However, the above methods obviously determine only the endpoint of the cell–chemotherapeutic drug interaction and do not enable continuous monitoring of the growth of drug-affected malignant cell populations *in vitro*.

Correspondence to V.D. Kravtsov at the Department of Cell Biology and Histology, Sackler School of Medicine, Tel Aviv University, Ramat-Aviv 69978, Tel Aviv, 39040 Israel.
Revised 31 May 1994; accepted 9 June 1994.

Incubated scanning microplate readers (e.g. THERMOmax™ Microplate Reader, Molecular Devices Corp., U.S.A. or iEMS Reader, Labsystems, Finland) have recently become commercially available. These machines are extensively utilised in microbiological laboratories for kinetic turbidimetric and chromogenic assays [9, 10]. To date, the use of incubated microplate readers for monitoring mammalian cell growth has not been possible because the incubated chamber of the reader does not preclude exposure of the cell microcultures to the ambient atmosphere, which results in evaporation of the warm fluid from the wells, escape of CO_2 from the media and possible contamination of the cell cultures with microorganisms.

We have developed a Microculture Kinetic Assay (MiCK assay) which overcomes the three problems of evaporation, sterility and pH maintenance in microcultures and allows at least a 3-day incubation of mammalian malignant cells in a microplate